Electronic Supplementary Material (ESI) for Journal of Materials Chemistry A.


# The high performance photoelectrochemical sensor for specific detection of $H_2O_2$ and glucose based on an organic conjugated microporous polymer

Qiqi Sun, ‡[a] Qi Liu, ‡[a] Wen Gao,[b] Chuanwang Xing,[a] Jingshun Shen,[a] Xue Liu,[a] Xia Kong,[c] Xiyou Li,[a] Yuexing Zhang *[d] and Yanli Chen *[a]

[a] *College of Science, School of Materials Science and Engineering, China University of Petroleum (East China), Qingdao 266580, PR China*

[b] *Department of Oncology, the Affiliated Hospital of Qingdao University, Qingdao 266580, PR China*

[c] *College of Chemical and Biological Engineering, Shandong University of Science and Technology,Qingdao 266580, PR China*

[d] *College of Chemistry and Chemical Engineering, Hubei University, Wuhan 430062 PR China*

** Corresponding authors at: College of Science, School of Materials Science and Engineering, China University of Petroleum (East China), Qingdao 266580, PR China (Y. Chen).*

*E-mail addresses: yanlichen@upc.edu.cn (Y. L. Chen), zhangyuexing@sdu.edu.cn (Y. X. Zhang)*

‡ *Q. Q. Sun and Q. Liu contributed equally to this work.*

## 1. Experimental section

*Materials*

Fluorine-doped tin oxide (FTO, 14Ω) conductive glasses were purchased from NGC. $Et_3N$ and THF were distilled from $CaH_2$ and Na, respectively. All other reagents and solvents were of reagent grade and used as received. Nafion (5 wt%) were purchased from Alfa Aesar Co. Ltd. $H_2O_2$ (30%) was purchased from Sinopharm Chemical Reagent Co., Ltd. CuI, $Pd(PPh_3)_2Cl_2$ 4-iodobenzaldehyde, pyrrole were purchased from Aladdin (Shanghai, China). 1,8-diazabicyclo[5.4.0]undec-7-ene (DBU), Glucose Oxidase (100 U/mg), 3,3′,5,5′-tetramethylbenzidine (TMB), *D*-Histidine, *p*-benzoquinone and terephthalic acid were purchased from Sigma-aldrich (Milwaukee, WI). Hydrogen peroxide ($H_2O_2$) solution, 30 wt.% in water and $H_2O_2$ assay kit were purchased from Innochem Co., Ltd (Beijing, China). All solutions were prepared with deionized (DI) water purified by Youpu Water Purification System (Chengdu Youpu Equipment Co., Ltd. China).

*Material Characterization*

MALDI-TOF mass spectra were recorded on a Bruker BIFLEX III ultrahigh-resolution Fourier transform ion cyclotron resonance (FT-ICR) mass spectrometer with alpha-cyano-4-hydroxycinnamic acid as the matrix. Elemental analysis was performed using a Vario EL III instrument. Thermogravimetric (TG) was performed on a simultaneous DSC-TGA SDT 650 analyzer under $N_2$ flowing with a 5 ℃ $min^{-1}$ heating rate. The $^{13}C$ CP/TOSS NMR spectra were recorded with a 4 mm MAS probe with a sample spinning rate of 3.0 kHz. IR spectra was recorded on a Hitachi U-3300 Fourier infrared spectrometer with KBr pellets. Raman spectroscopy of the samples was measured with a laser Raman microscope system (Nanophoton RAMANtouch) excited with 532 nm. X-ray diffraction (XRD) analysis was performed on a Rigaku Ultima IV X-ray diffractometer using a Cu Kα source (40 kV, 40 mA, λ = 0.154056 nm). The morphology and structure of the materials were measured by field-emission scanning electron microscope (SEM, Quant 250FEG) and high resolution transmission electron microscope (HRTEM, JEM-2100F) at 200 kV. $N_2$ adsorption-desorption isotherms were

analyzed through a Micromeritics ASAP 2060 analyzer at 77 K and the specific surface area of the materials were calculated based on the Brunauer-Emmett-Teller (BET) method, the total pore volume was estimated from single point adsorption at a relative pressure $P/P_0$ of 0.995 and the pore size distributions were calculated by means of NLDFT method. Ultraviolet Photoelectron Spectroscopy (UPS) data were collected with a homemade He lamp source which produces a resonance line He I and He II under sample biases (1 V). Ultraviolet-visible spectroscopy (UV-vis) and UV-vis diffuse reflection spectra (DRS) were operated on a Hitachi U-3900 spectrophotometer. Photoluminescence spectrum (PL) was recorded on a Hitachi F-7000 fluorescence spectrophotometer. The emission quantum yields were collected on FLS980 (Edinburgh instrument Ltd, England) under excitation wavelength of 430 nm for PorPor-CMP and PorPc-CMP, 600 nm for PcPc-CMP with an integrated sphere attachment and $BaSO_4$ used as the reference. Time-resolved photoluminescence spectra was collected on FLS980 (Edinburgh instrument Ltd, England) with an excitation wavelength of 340 nm. The optical profile were collected on ZYGO newview7100. The Atomic Force Microscopy (AFM) were collected on Park systems NX-Wafer.

*Preparation of CMPs*

Preparation of PorPor-CMP: The 5, 10, 15, 20-tetrakis(4-iodophenyl)porphyrin (TIPP) and 5,10,15,20-tetrakis(4-ethynylphenyl)porphyrin (TEPP) were prepared according to published procedures,[1,2] and characterized by mass spectrometry and elemental analysis, Scheme S1 and Fig. S3. The PorPor-CMP was synthesized through polycondensation via a Sonogashira–Hagihara coupling reaction, Scheme S1. In a typical synthesis, a mixture of TEPP (142 mg, 200 mmol) and TIPP (224 mg, 200 mmol) into $Et_3N$/THF (40 / 80 mL) with CuI (2.0 mg, 10.5 mmol) and $Pd(PPh_3)_2Cl_2$ (3.0 mg, 15.9 mmol) as co-catalysts was heated to 65 ℃ under a $N_2$ atmosphere for 48 h. After the mixture cooled to room temperature, the product was collected by filtration; washed with $H_2O$, DMF, toluene, THF, $CHCl_3$, and $CH_3OH$ in order. Then the wet sample was washed by Soxhlet extraction for 24 h with THF, methanol, and acetone as solvents, respectively, to remove the unreacted TEPP, TIPP. Finally, the generate bulk PorPor-

CMP was dried in a vacuum oven at 80 ℃ for 12 h, the yield is 87% (229mg, yield % = theoretical mass/actual mass %).

Preparation of PcPc-CMP: The 2(3),9(10),16(17),23(24)-tetra(iodo)phthalocyanine ($H_2$[Pc(I)$_4$]), 2(3),9(10),16(17),23(24)-tetra(ethynyl)phthalocyanine ($H_2$[Pc(ethynyl)$_4$]), were prepared according to published procedures,[3,4] and characterized by mass spectrometry and elemental analysis, Scheme S1 and Fig. S3. The PcPc-CMP was synthesized through polycondensation via a Sonogashira–Hagihara coupling reaction, Scheme S1. In a typical synthesis, a mixture of $H_2$[Pc(ethynyl)$_4$] (122 mg, 200 mmol) and $H_2$[Pc(I)$_4$] (204 mg, 200 mmol) into $Et_3N$/THF (40 / 80 mL) with CuI (2.0 mg, 10.5 mmol) and Pd($PPh_3$)$_2Cl_2$ (3.0 mg, 15.9 mmol) as co-catalysts was heated to 65 ℃ under a $N_2$ atmosphere for 48 h. After the mixture cooled to room temperature, the product was collected by filtration; washed with $H_2O$, DMF, toluene, THF, $CHCl_3$, and $CH_3OH$ in order. Then the wet sample was washed by Soxhlet extraction for 24 h with THF, methanol, and acetone as solvents, respectively, to remove the unreacted $H_2$[Pc(ethynyl)$_4$], $H_2$[Pc(I)$_4$]. Finally, the generate bulk PcPc-CMP was dried in a vacuum oven at 80 ℃ for 12 h, the yield is 83% (186mg, yield % = theoretical mass/actual mass %).

*Density Functional Theory (DFT) Calculation*

The initial crystal structures of PorPor-CMP, PorPc-CMP, and PcPc-CMP are built with Materials Visualizer interface of BIOVIA Materials Studio 2017 (17.2) and then these structures together with the cell unit were optimized. The PerdewBurke-Ernzerh exchange-correlation functional of generalized gradient approximation (GGA-PBE) with Grimme's default DFT-D parameters was used. The double-numeric with polarization functions basis set (DNP) was chosen. All calculations were performed using the DMol$^3$ module of BIOVIA Materials Studio 2017 (17.2). The optimized crystals are C222 space group with a = b = 27.7 Å and α = β= γ= 90º for PorPor-CMP,

P2 space group with a = b = 36.7 Å and α = β= γ= 90º for PorPc-CMP, and P2/M space group with a = 17.0 Å and b = 20.2 Å and α = β= γ= 90º for PcPc-CMP. c axis was set to long enough to avoid interactions between layers (about 20 Å after optimization). The convergence criteria for structure optimization were set to: (a) a SCF tolerance of $1 \times 10^{-5}$ hartree, (b) an energy tolerance of $1 \times 10^{-5}$ hartree, (c) a maximum force tolerance of $2 \times 10^{-3}$ hartree/Å; and (d) a maximum displacement tolerance of $5 \times 10^{-3}$ Å, (e) thermal smearing of 0.010 Ha, (f) Monkhorst-Pack grid k-points of 1 ×1 × 1. Based on the optimized crystal structures, energies and electron properties were performed with similar setting up as optimization except that the energy tolerance was increased to $1 \times 10^{-6}$ hartree and k-points was changed to 4×4×2.

*Anti-Interference, Repeatability, and Stability Test*

Anti-Interference test of PorPc-CMP sensor for $H_2O_2$ and glucose was performed by adding L-tyrosine, L-tryptophan, L-arginine, B-alanine, L-asparaginic acid, D-cysteine, L-histidine, guanine, adenine, cholesterol, glucose/ galactose, dopamine, bisphenol A, catechinic acid, salicylic acid, acetaminophen, trioxypurine, ascorbic acid, citric acid, rutin hydrate, $Na^+$, $K^+$, $Mg^{2+}$, $Fe^{3+}$, $Zn^{2+}$, and $Ca^{2+}$ gradually ([Inf]/[$H_2O_2$] or [Glu] = 10 : 1). The repeatability was tested through detecting 1 and $10 \times 10^{-6}$ M glucose with five PorPc-CMP sensors prepared in the same manner. Long-term stability testing is concerned with applying the prepared PorPc sensor for detecting glucose before and after being stored in air for 180 days without being used.

*Peroxidase-like Activity Assay*

In a typical procedure, 200 μL of CMPs (0.5 mg $mL^{-1}$), 200 μL of $H_2O_2$ (5 mM), 200 μL of TMB (0.5 mM), and 1.4 mL Tris-HCl solution (0.1 M, pH=7.0) were mixed together and kept in a total volume of 2 mL. The solutions were irradiated under the wavelength of 420-430 nm LED lamp-house. After 1 min, absorbance of the solution was obtained on a spectrophotometer.

*ROS Scavenger Quenching and Identifying Experiments*

The ROS quenching experimental process was similar to the peroxidase-like activity of three CMPs (50 μg/mL PorPor-CMP/PorPc-CMP/PcPc-CMP, 0.5 mM $H_2O_2$ and 0.05 mM TMB), apart from adding quenching agents ($CH_3OH$, *D*-histidine and *p*-benzoquinone) (10 mM) to the different systems.

The hydroxyl radical (•OH) generated by CMPs + $H_2O_2$ were investigated by measuring the respective fluorescence of 2-hydroxyterephthalic acid, which was generated by the reaction of TA with •OH. In this procedure, 200 μL of CMPs (0.5 mg $mL^{-1}$) were added into 1.8 ml Tris-HCl solution containing TA (0.5 mM) and $H_2O_2$ (0.5 mM), incubate 1 min under LED lamp, and then, the fluorescence intensities of 2-hydroxyterephthalic acid at 426 nm were monitored.

*The optimization of Nafion dosage for PEC sensor*

In order to establish a better sensor, the Nafion dosage was investigated using PorPc-CMP. As shown in Fig. S1A, the constructed photoelectrodes with too high (>90 μL) or too low (<10 μL) amount of nafion have very poor activity and show similar activity between 40 and 70 μL. Comprehensive consideration, in order to minimize the impact of Nafion on the porosity of the polymer material, we chose 40 μL of Nafion dosage.

In addition, we use another method (method-2), first drop the polymer material onto the electrode surface, and then drop a thin layer of Nafion solution. This method can significantly reduce the impact of Nafion solution on the pores of the material. The test found that this is not much different from the method (method-1) used in this manuscript, although it shows a slightly higher activity, but the stability is worse, as shown in Fig S1B and S1C. In summary, a proper amount of Nafion will not reduce the activity of the photoelectrode, but also helps to improve the stability of the photoelectrode.

*The optimization for pH value of Tris-HCl solution to $H_2O_2$ PEC sensing*

In order to establish a better monitoring environment, the influences of the pH were investigated using PorPc-CMP, Fig. S10. As shown in Fig. S10, the photocurrent response increased from pH=3.0 to pH=7.0, and then dropped sharply at pH=8.0. Therefore, the optimum pH is 7.0. It shows that the system is close to the human environment and is beneficial to the detection of the human environment.

*The optimization for pH value of Tris-HCl solution to glucose PEC sensing*

In order to establish a better monitoring environment, the influence of the pH value was investigated using PorPc-CMP, Fig. S19. As shown in Fig. S19, the photocurrent response increased from pH=3.0 to pH=7.0, stayed steady between pH =6 to pH =7 and then dropped sharply at pH=8.0. Therefore, the optimum pH is 7.0. It shows that the system is close to the human environment and is beneficial to the detection of the human environment.

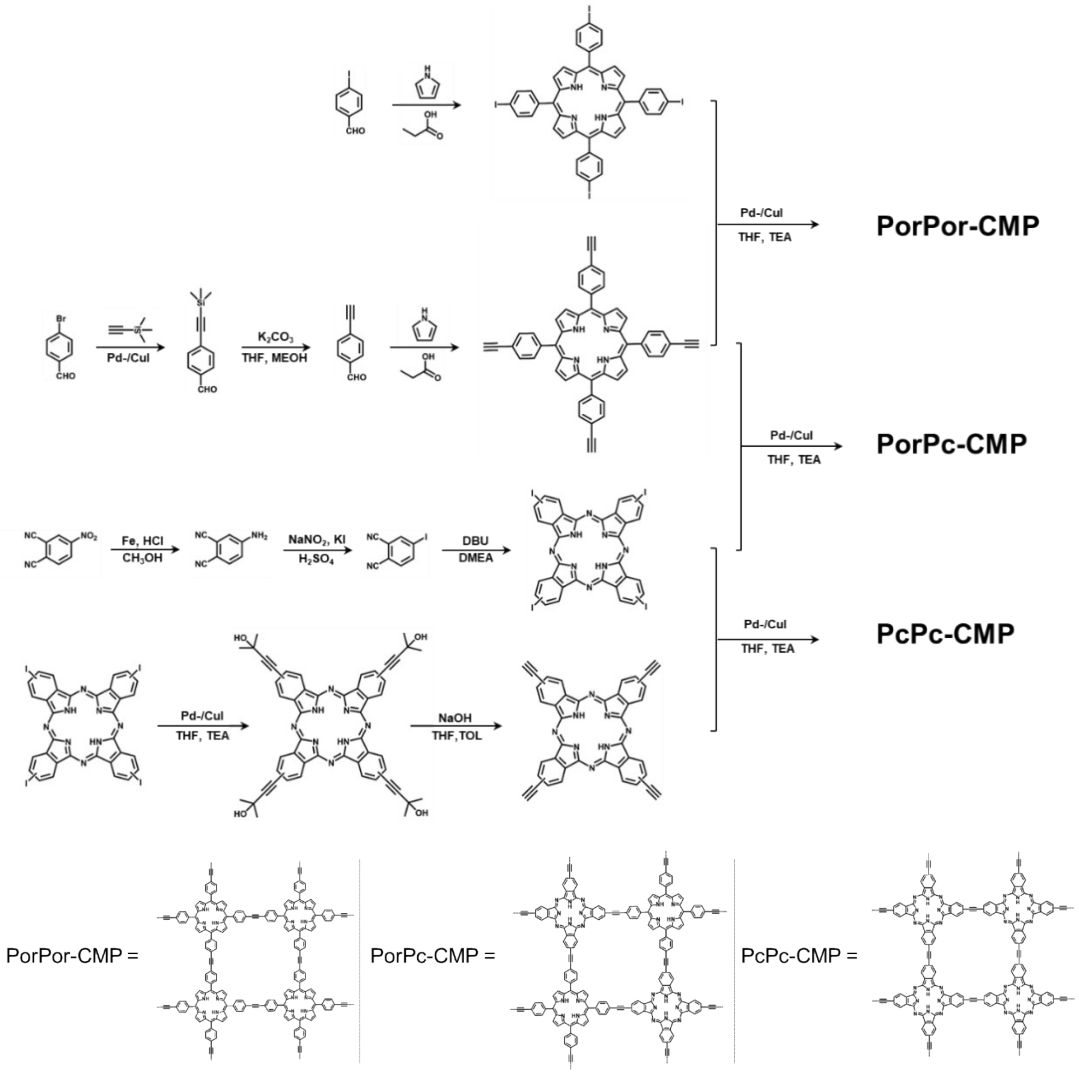


**Scheme S1** Synthesis route to PorPor-CMP, PorPc-CMP, and PcPc-CMP.

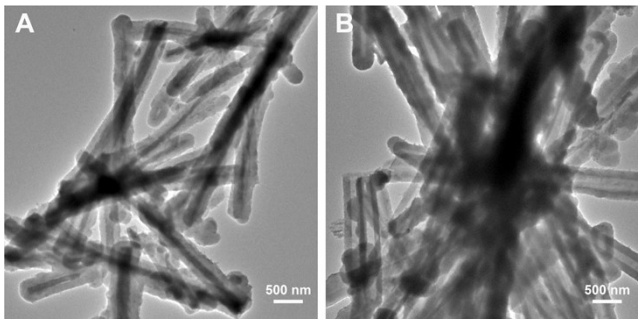


**Fig. S1** The TEM image of PorPc-CMP solid tube befor washing (A) and hollow tube after washing (B) by Soxhlet method

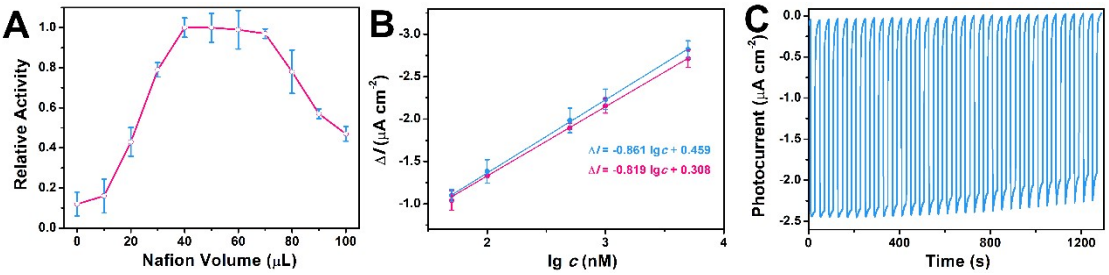


**Fig. S2** The relative activity of PorPc-CMP electrode with different dosage of Nafion (A), Photocurrent responses of two types of PorPc-CMP sensors obtained by using method-1 (Red) and method-2 (Blue) for $H_2O_2$ in the range of 0.05-5 mM (B), Photocurrent response of the PEC sensor fabricated by method-2 under periodic light irradiation (C).

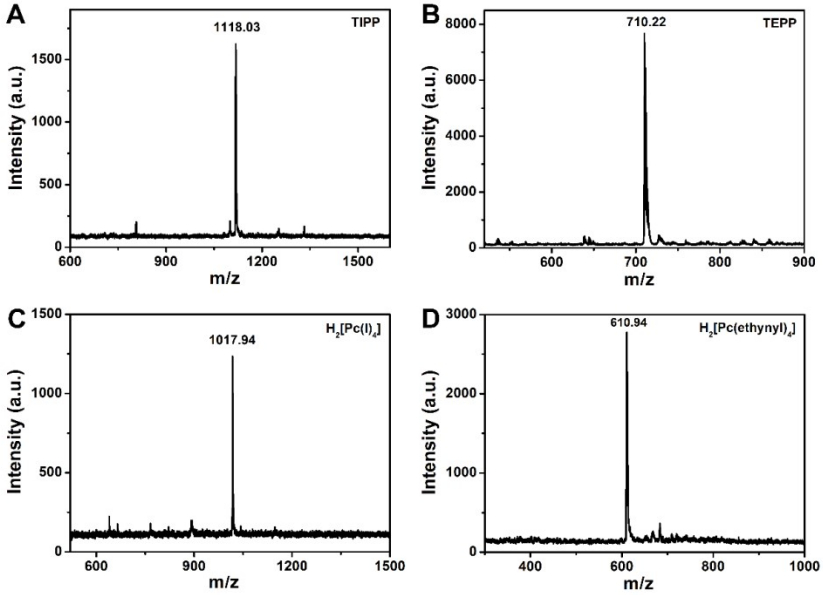


**Fig. S3** MALDI-TOF mass spectrum of TIPP (A), TEPP (B), $H_2[Pc(I)_4]$ (C), and $H_2[Pc(ethynyl)_4]$ (D).
TIPP: MALDI-TOF MS: calcd. for $C_{44}H_{26}N_4I_4$ ($M^+$): 1117.83; found m/z 1118.03 (Fig. S1A). Elemental analysis: Calcd for $C_{44}H_{26}N_4I_4$: C 47.26; H 2.34; N 5.01; Anal. found C 47.37; H 2.67; N 5.47. TEPP: MALDI-TOF MS: calcd. for $C_{52}H_{30}N_4$ ($M^+$): 710.25; found m/z 710.22 (Fig. S1B). Elemental analysis: Calcd for $C_{52}H_{30}N_4$: C 87.86; H 4.25; N 7.88; Anal. found C 87.21; H 4.67; N 8.12. $H_2[Pc(I)_4]$: MALDI-TOF MS: calcd. for $C_{34}H_{14}N_8I_4$ ($M^+$): 1017.75; found m/z 1017.94 (Fig. S1C). Elemental analysis: Calcd for $C_{34}H_{14}N_8I_4$: C 37.75; H 1.39; N 11.01; Anal. found C 37.42; H 1.57; N 10.89. MALDI-TOF MS: calcd. for $C_{40}H_{18}N_8$ ($M^+$): 610.17; found m/z 610.94 (Fig. S1D). Elemental analysis: Calcd for $C_{40}H_{18}N_8$: C 78.68; H 2.97; N 18.35; Anal. found C 78.81; H 3.26; N 17.93.

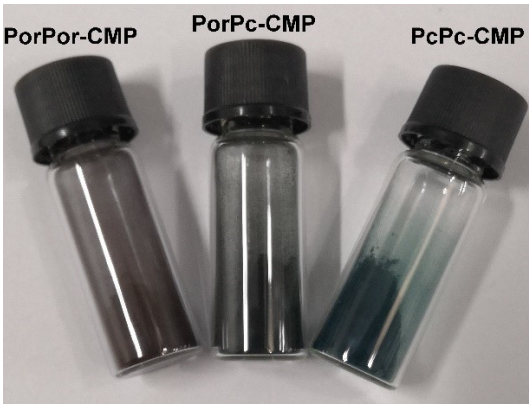


**Fig. S4** Powder samples of three CMPs.

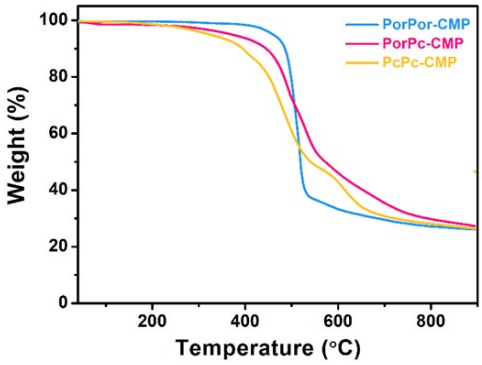


**Fig. S5** TGA of PorPor-CMP, PorPc-CMP, and PcPc-CMP.

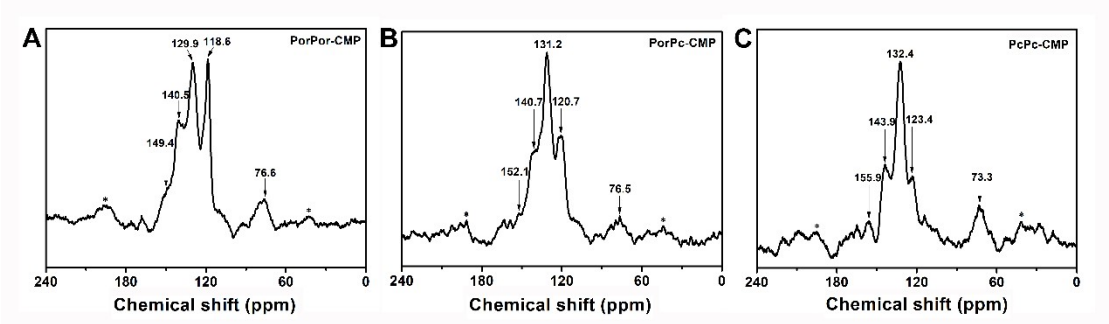


**Fig. S6** $^{13}$C CP/MAS NMR spectra of PorPor-CMP (A), PorPc-CMP (B), and PcPc-CMP (C).

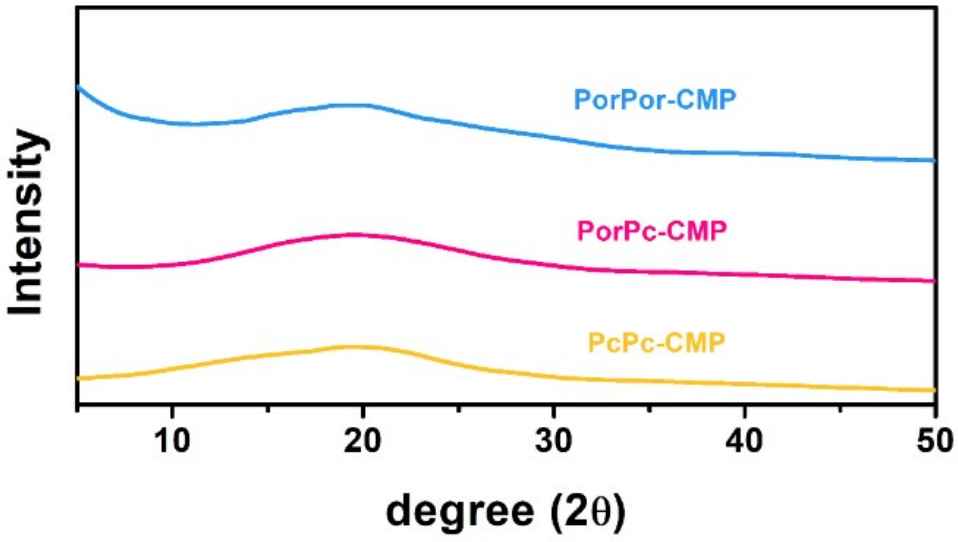


**Fig. S7** PXRD patterns of PorPor-CMP, PorPc-CMP, and PcPc-CMP.

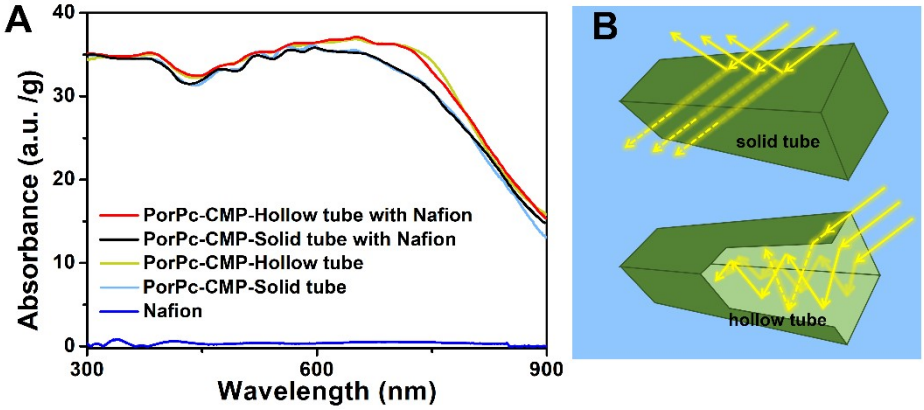


**Fig. S8** UV-vis DRS of PorPc-CMP-solid tube and hollow tube, and nafion-treated PorPc-CMP-solid tube and hollow tube, and nafion film (A)[a] A schematic light pathway illustration of PorPc-CMP-solid tube and hollow tube (B)

[a] In order to make the comparison in **Fig. S8A** more rigorous, we designed the following experiment. First, two groups of the PorPc-CMP solid tubes (each 50 mg) were accurately weighed and recorded as sample A and sample B respectively. Then, the rigorously washing by Soxhlet method for sample A was carried out and sample B remained constant. At this point, the weights of PorPc-CMP in the two groups of samples A and B were approximately equal, followed by treatment with nafion, drying and UV-vis DRS testing.

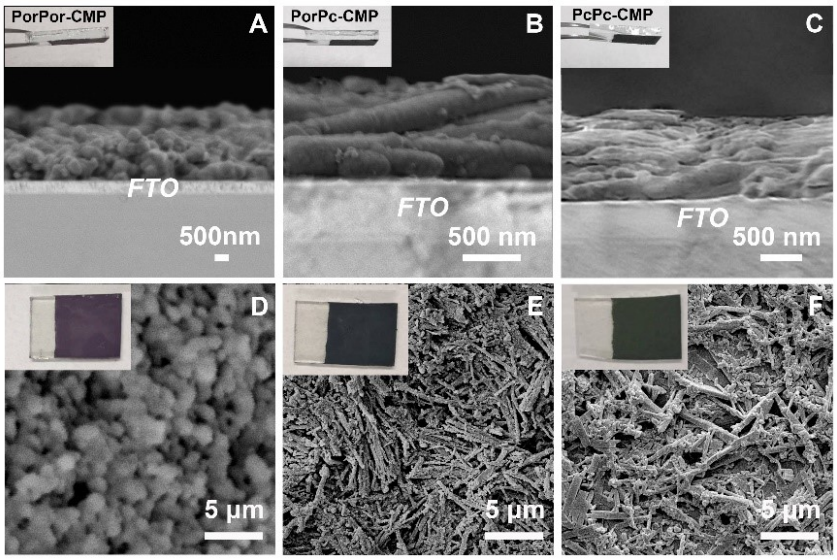


**Fig. S9** The photographs and SEM images (Side views) (A-C) and (Top views) (D-F) of the three membranes on FTO electrodes, respectively.

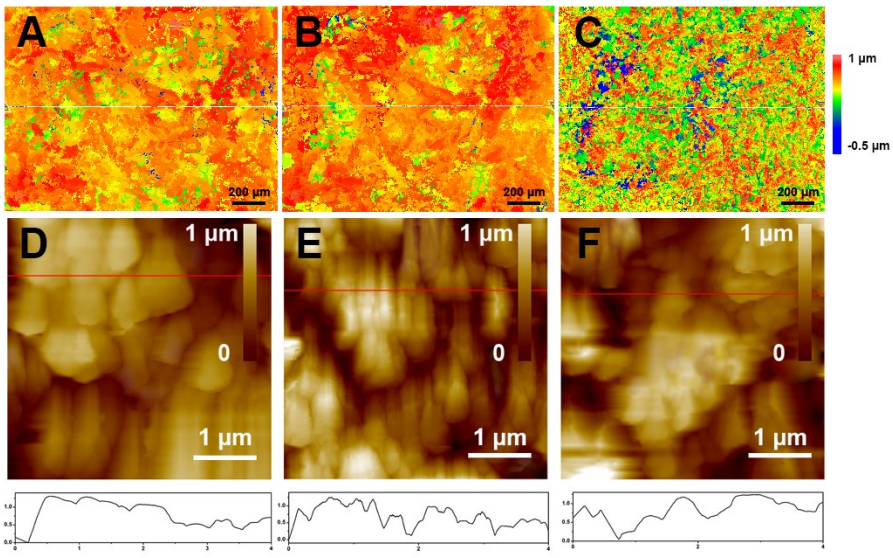


**Fig. S10** The optical profile and AFM images of the PorPor-CMP (A, D), PorPc-CMP (B, E) and PcPc-CMP (C, F) membranes, respectively.

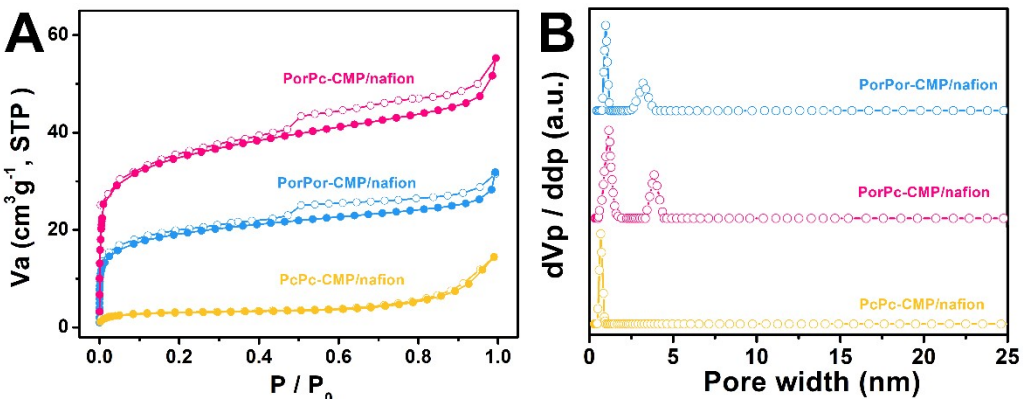


**Fig. S11** $N_2$ adsorption-desorption isotherms(77·K) of nafion-treated PorPor-CMP, PoPc-CMP, and PcPc-CMP(A)and the pore-size distribution of nafion-treated CMPs (B).

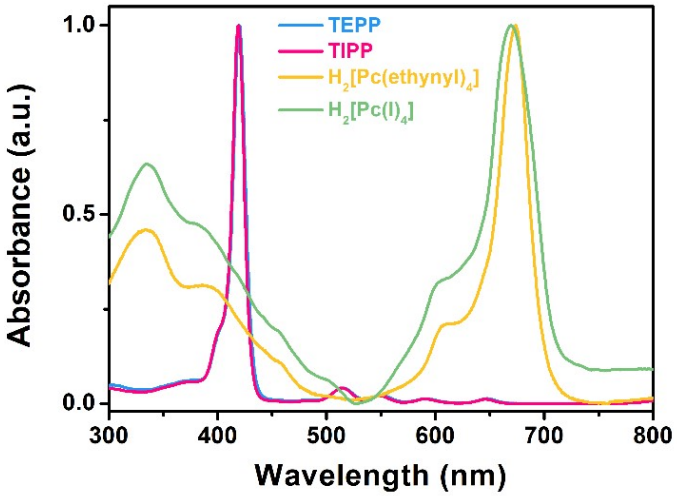


**Fig. S12** UV-vis absorption spectra of corresponding monomers in DMF solution.

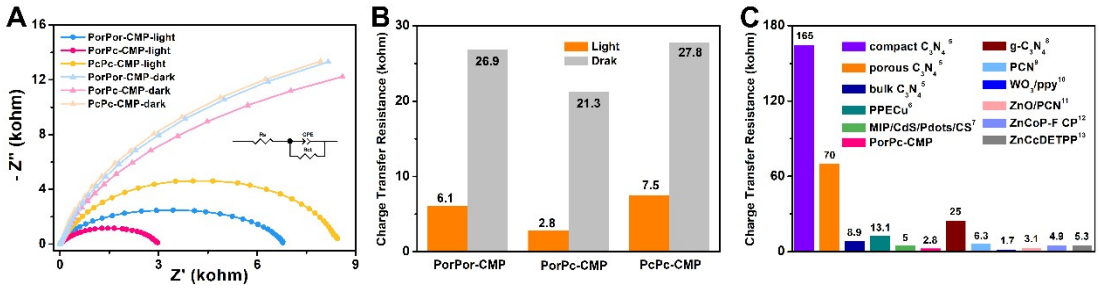


**Fig. S13** EIS of PorPor-CMP, PorPc-CMP, and PcPc-CMP under light and dark (A), the $R_{ct}$ of PorPor-CMP, PorPc-CMP, and PcPc-CMP under light and dark (B), the $R_{ct}$ of PorPc-CMP and other polymers from literatures under light (C). The superscript number in the name of each material represents the number of references. [5-13]

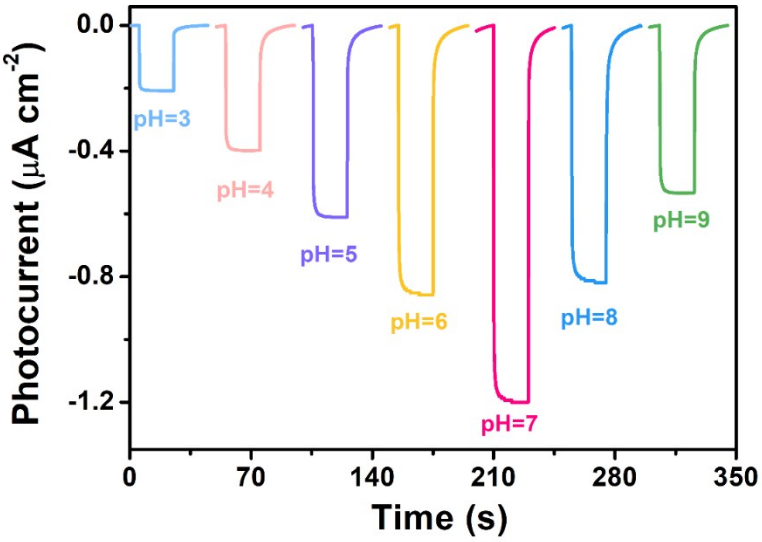


**Fig. S14** The photocurrent response of PorPc-CMP in different pH.

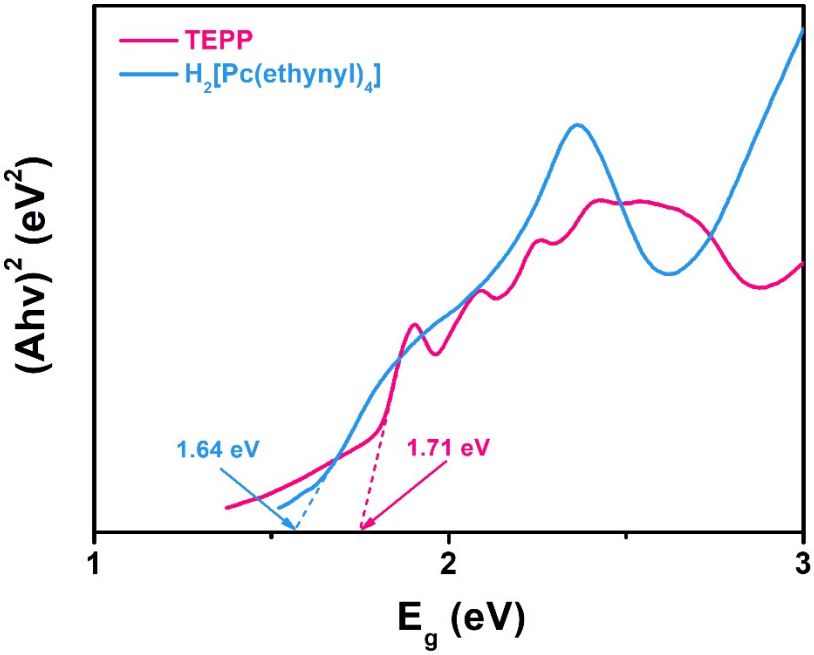


**Fig. S15** Tauc plots of TEPP and $H_2$[Pc(ethynyl)$_4$]

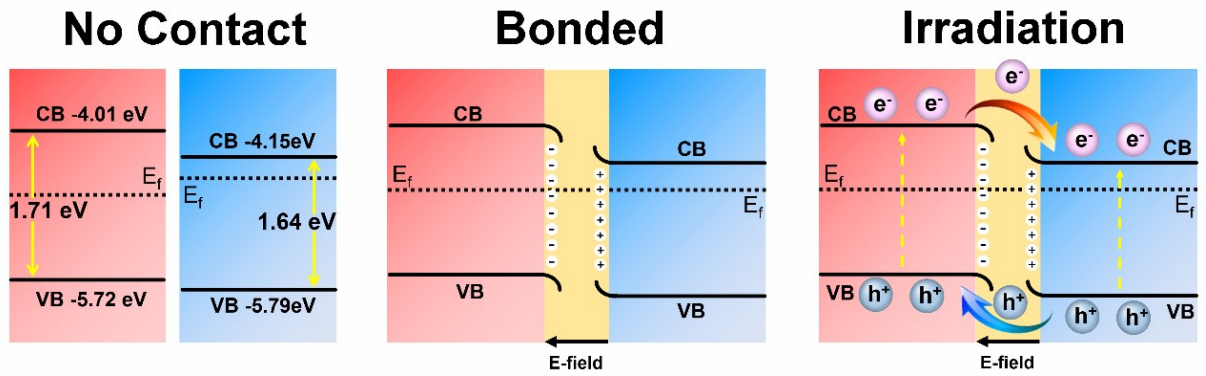


**Fig. S16** Schematic energy band diagrams of TEPP and $H_2$[Pc(ethynyl)$_4$].

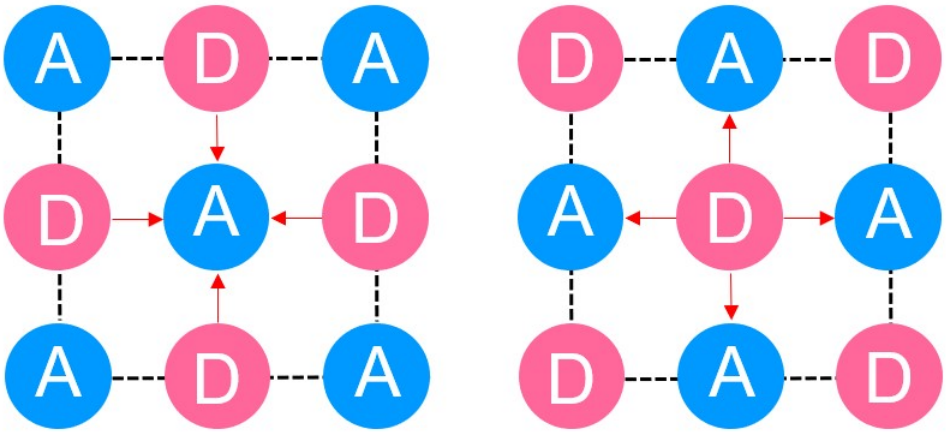


**Fig. S17** Schematic diagram of multi-channel electronic transmission between Donor (TEPP: carmine) and Acceptor ($H_2$[Pc(ethynyl)$_4$]: azure).

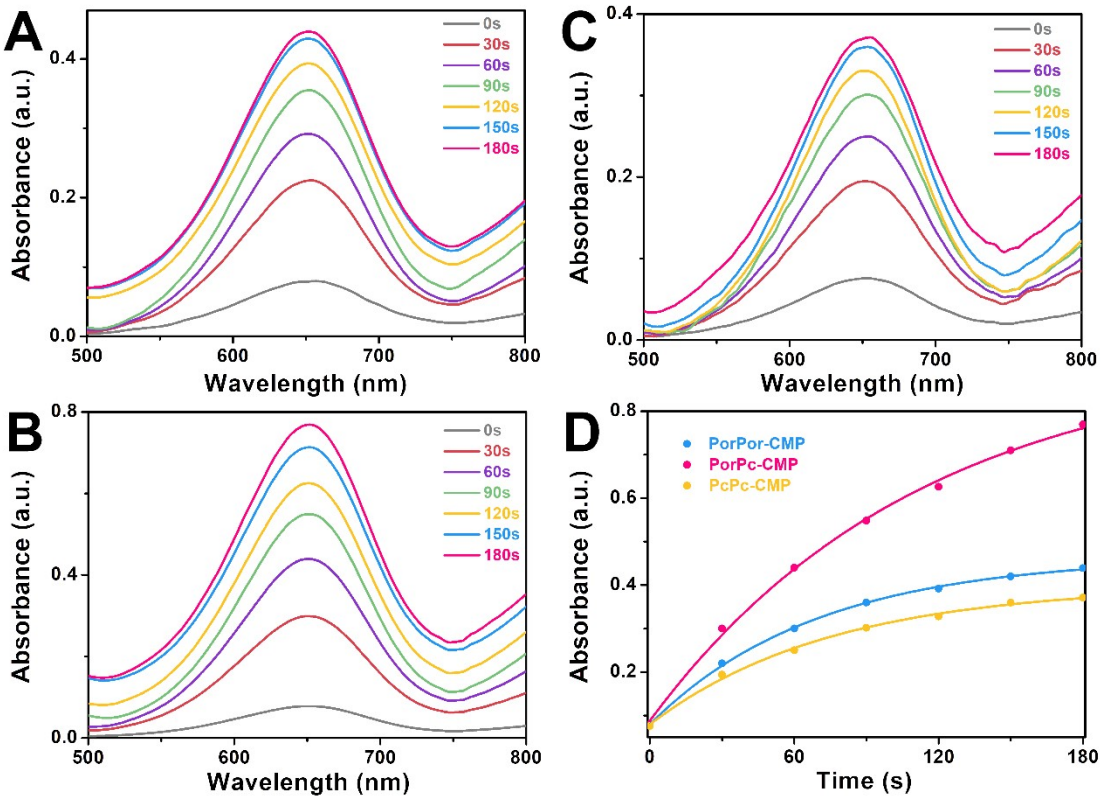


**Fig. S18** UV-vis spectra of the PorPor-CMP + $H_2O_2$ + TMB system (A), PorPc-CMP + $H_2O_2$ + TMB system (B), and PcPc-CMP + $H_2O_2$ + TMB system (C) for different times. Effect of time on the absorbance changes of the above three systems (D).

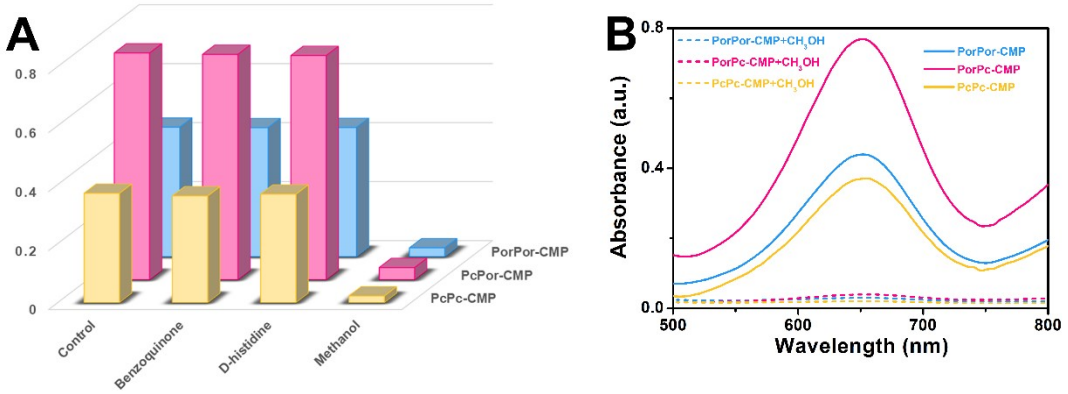


**Fig. S19** The absorbance of the TMB+$H_2O_2$+CMPs reaction system in the pressure of *p*-benzoquinone ($O_2^{\bullet-}$ scavenger), *D*-histidine ($^1O_2$ scavenger), and methanol ($^\bullet$OH scavenger) (A). The UV-vis spectra of the TMB+$H_2O_2$+CMPs reaction system with or without methanol (B).

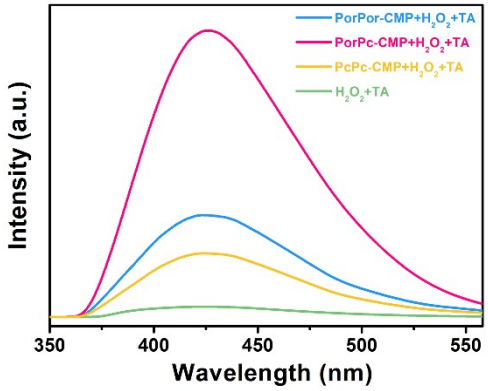


**Fig. S20** Fluorescence spectroscopy of the TA + $H_2O_2$ and TA + $H_2O_2$ + CMPs systems ($\lambda_{max}$ = 312 nm)

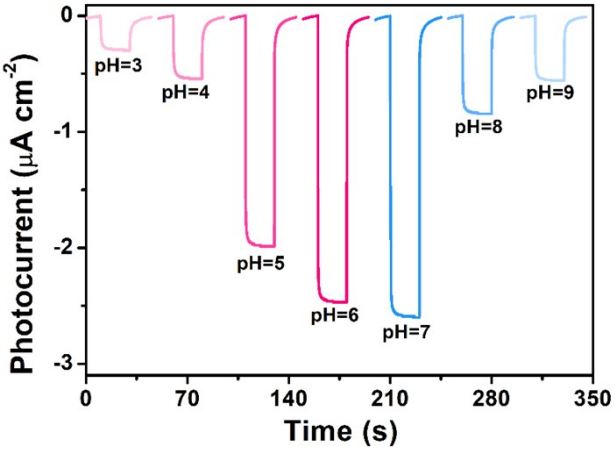


**Fig. S21** The photocurrent response for 0.05 μM glucose of PorPc-CMP in different pH.

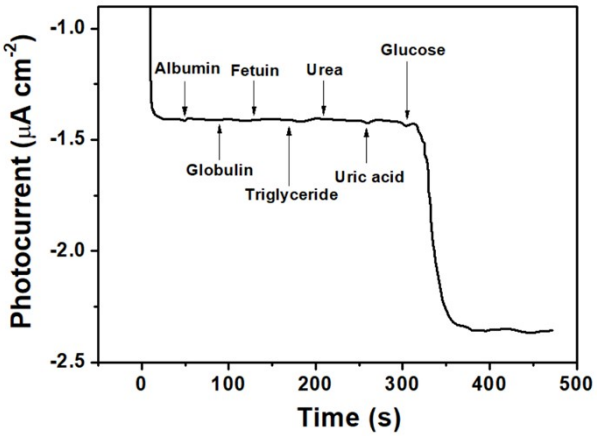


**Fig. S22** Photocurrent responses of PorPc-CMP PEC sensor with successive additions of 0.05 μM glucose and different analytes (albumin: 100mg/ml, globulin: 50 mg/ml, fetuin: 45mg/ml, triglyceride, urea and uric acid: 1mM) into pH=7.0 Tris-HCl solution and glucose oxidase

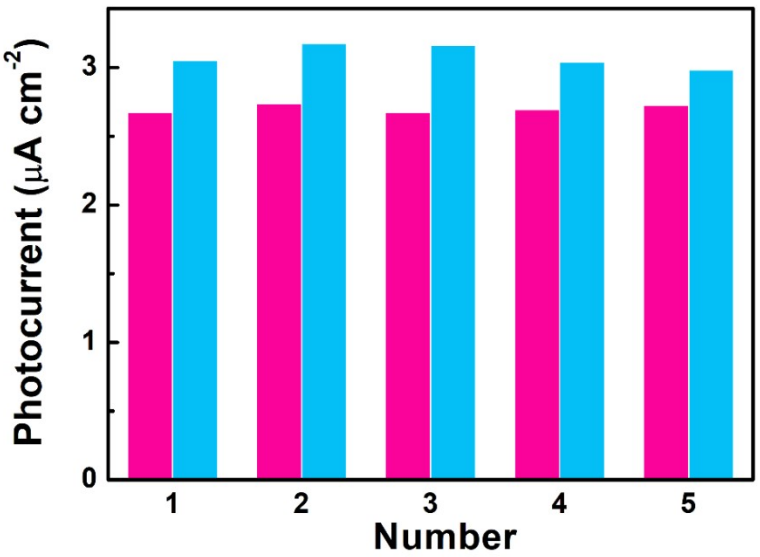


**Fig. S23** Photocurrent responses of five PorPc-CMP sensors to 1 and 10 μM glucose.

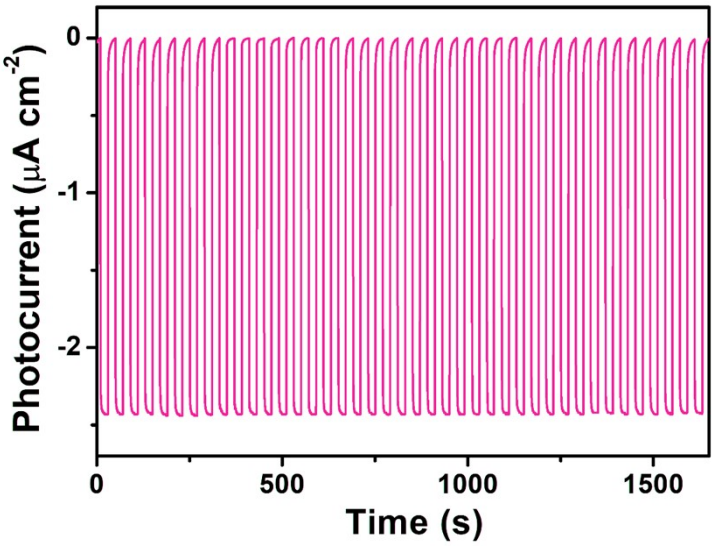


**Fig. S24** Response of the PEC sensor during continuous detection of 0.5 μM glucose under periodic light irradiation for 1600 s.

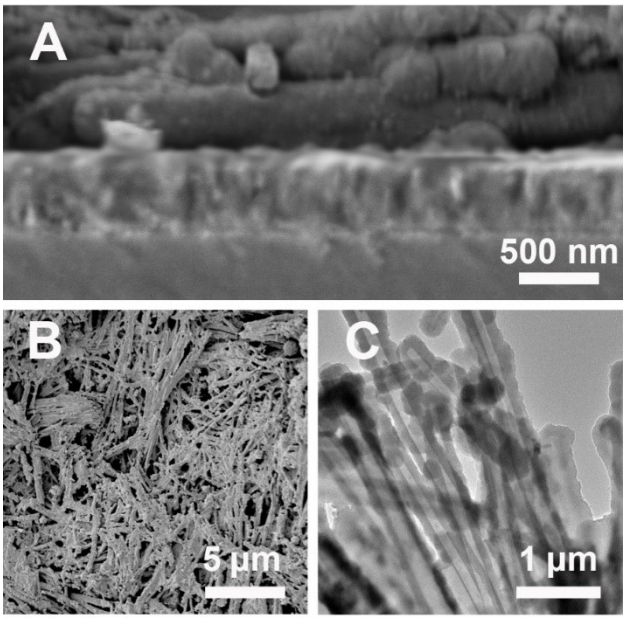


**Fig. S25** The SEM images of side (A) and top view (B) for PorPc-CMP and the TEM images of PorPc-CMP after cyclic test (C)

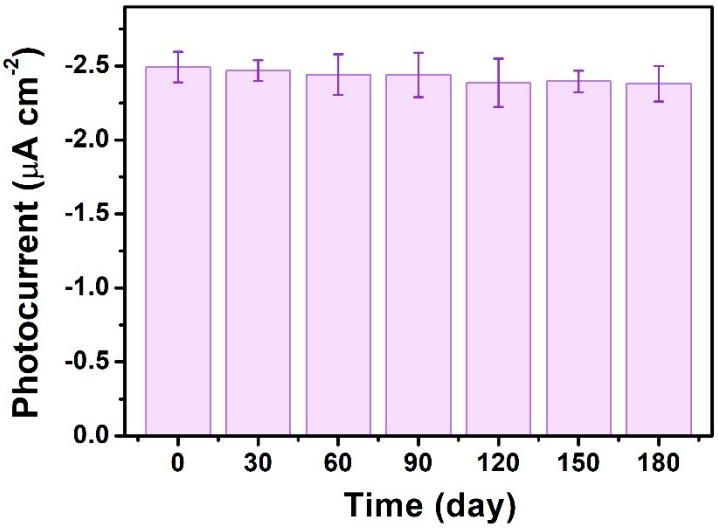


**Fig. S26** Stability over 180 days for the detection of 0.5 μM glucose. (RSD=1.8%)

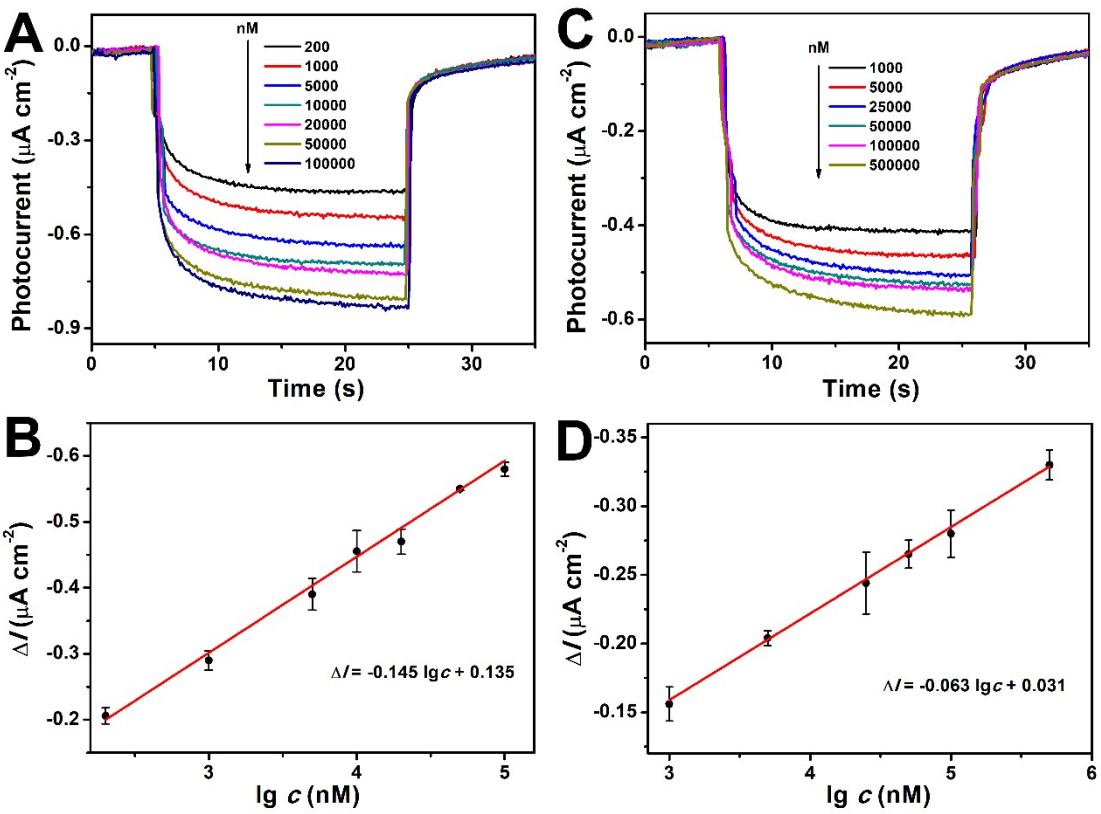


**Fig. S27** Photocurrent responses of PorPc-CMP PEC sensor in different $H_2O_2$ (A) and glucose (B) concentration with two-electrode system. The relationship between photocurrent and $H_2O_2$ (C) /glucose (D) concentration.

**Table S1**. UV–vis absorption spectral data of *free-base* porphyrins TEPP, TIPP and phthalocyanine $H_2Pc(ethynyl)_4$, $H_2Pc(I)_4$ in DMF (l).

| Compound | Soret Band | Q bands |
|---|---|---|
| TEPP (*l*) | 416 | 516, 551, 591, 648 |
| TIPP (*l*) | 420 | 515, 549, 591, 646 |
| $H_2Pc(ethynyl)_4$ (*l*) | 334, 387 | 609, 674 |
| $H_2Pc(I)_4$ (*l*) | 335, 379 | 602, 670 |

**Table S2**. Fluorescence spectra data of monomers and the three CMPs

| Compound | Porphyrin Emissions | Phthalocyanine Emissions |
|---|---|---|
| TEPP | 628 | – |
| $H_2Pc(ethynyl)_4$ | – | 725 |
| PorPor-CMP | 631 | – |
| PorPc-CMP | 634 | 725 |
| PcPc-CMP | – | 726 |

**Table S3** Fitted decay time of these polymers.

| CMP | **Fitted decay time[a]** | | |
|---|---|---|---|
| | $\tau_1$ | $\tau_2$ | $\tau_3$ |
| PorPor-CMP | 0.3477 | 4.1357 | 16.3826 |
| PorPc-CMP | 0.2794 | 1.8600 | 8.0308 |
| PcPc-CMP | 0.7212 | 8.1762 | 131.3664 |

[a] Obtained from fluorescence decay spectrum of the polymers recorded in solid state.

**Table S4** Comparison of the $H_2O_2$ sensors using various methods

| Electrode composition | Method | Liner range (μM) | LOD (μM) | Refs. |
|---|---|---|---|---|
| FeTSPc-GR-Nafion/SPE | Electrochemical | 0.2-5000 | 0.08 | 14 |
| TOAB/ZnPp-$C_{60}$/GCE | Electrochemical | 35-3400 | 0.27 | 15 |
| Triple-decker/GO/ITO | Electrochemical | 0.05-1800 | 0.017 | 16 |
| GC/(Co-TCPP(Fe))$_5$ | Electrochemical | 0.4-50 | 0.15 | 17 |
| (FePc-CP NSs)$_4$ | Electrochemical | 0.05-1800 | 0.017 | 3 |
| NiO/graphene nanocomposite | Electrochemical | 250-475 | 0.77 | 18 |
| ZnO/$Co_3O_4$/$NiCo_2O_4$/Ni foam | Electrochemical | 0.2–2400 | 0.16 | 19 |
| GQDs/AgNPs | Colorimetric | 0.1–100 | 0.033 | 20 |
| $H_2$TCPP-ZnS | Colorimetric | 10-60 | 15.8 | 21 |
| Por-$NiCo_2S_4$ | Colorimetric | 20-1000 | 10.06 | 22 |
| PbS NPs/RGO/NiO nanosheet | PEC | 0.05-100 mM | 18 | 23 |
| ITO-$TiO_2$ IOPCs– CdS:Mn | PEC | 63-4000 | 19 | 24 |
| ITO/PbS/$Co_3O_4$ nanofilm | PEC | 5-500 | 1.2 | 25 |
| g-$C_3N_4$/$P_3$HT | PEC | 1-800 | 0.38 | 26 |
| $BiVO_4$-rGO | PEC | 0.1-2000 | 0.03 | 27 |
| PorPor-CMP | PEC | 1-100 | 0.413 | This work |
| PorPc-CMP | PEC | 0.05-100 | 0.013 | This work |
| PcPc-CMP | PEC | 1-100 | 0.56 | This work |

**Table S5** The calculated charges of TEPP and $H_2$[Pc(ethynyl)$_4$] in PorPc-CMP by Mulliken method and Hirshfeld method

| Compound | Mulliken charges | Hirshfeld charges |
|---|---|---|
| TEPP | 0.079 | 0.0693 |
| $H_2$[Pc(ethynyl)$_4$] | -0.084 | -0.0594 |

**Table S6** Comparison of the glucose sensors using various method

| Electode composition | Method | Liner range (μM) | LOD (μM) | Refs. |
|---|---|---|---|---|
| PAA-rGO/VS-PANI/$LuPc_2$-MFH | Electrochemistry | 2000-12000 | 25 | 28 |
| CoPc/IL/G/SPCE/PADs | Electrochemistry | 10-5000 | 0.67 | 29 |
| PAA-VS-PANI/GPL-FePc/GOx-CH | Electrochemistry | 1000-20000 | 6.4 | 30 |
| Al doped ZnO (AZO) thin film | Photoluminescence | 20-20000 | 6.9 | 31 |
| MGO-P(4-VBA) | Electrochemistry | 1–15 mM | 39 | 32 |
| TCS-$TiO_2$ nanorods | Electrochemistry | 5-1320 | 2 | 33 |
| GOx/Au-g-$C_3N_4$ | Electrochemiluminescence | 0.5-8000 | 0.05 | 34 |
| SDS-$MoS_2$ NPs | Colorimetry | 5-500 | 0.57 | 35 |
| N-GQDs | Colorimetry | 25-375 | 16 | 36 |
| Au NPs/Cu-TCPP(M) | Colorimetry | 10-300 | 8.5 | 37 |
| Fe SSN | Colorimetry | 0-60 | 2.1 | 38 |
| PbS NPs/RGO/NiO nanosheet | PEC | 0.1-100000 | 0.053 | 23 |
| GOx/BiOI/NiO | PEC | 5-10000 | 1.6 | 39 |
| ZnS/$CuInS_2$/$TiO_2$/ITO | PEC | 0.1-5000 | 0.035 | 40 |
| Polymer phenylethnylcopper | PEC | 0.5–5000 | 0.16 | 41 |
| BiOI/NiO nanofilm | PEC | 5-10000 | 1.6 | 42 |
| PorPc-CMP | PEC | 0.05-5000 | 0.027 | This work |

## References


[1] W. Liu, Y. Hou, H. Pan, W. Liu, D. Qi, K. Wang, J. Jiang and X. Yao, *J. Mater. Chem. A*, 2018, **6**, 8349.

[2] J. Tian and W. Zhang, *Prog. Polym. Sci*., 2019, **95**, 65-117

[3] W. Liu, H. Pan, C. Liu, Ch. Su, W. Liu, K. Wang, and J. Jiang, *ACS Appl. Mater. Interfaces*,2019, **11**, 11466−11473

[4] W. Liu, Ch.Wang, L. Zhang, H. Pan, W. Liu, J. Chen, D. Yang, Y. Xiang, K. Wang, J. Jiang and X. Yao, *J. Mater. Chem. A*, 2019, **7**, 3112

[5] Q. Ruan, MK. Bayazit, V. Kiran, J. Xie, Y Wang and J. Tang, *Chem. Commun.*, 2019, **55**, 7191-7194

[6] Z. Wei, J. Hu, K. Zhu, W. Wei, X. Ma, and Y. Zhu, *Appl. Catal. B Environ*., 2018, **226**, 616-623

[7] L. Mao, M. Gao, X. Xue, L. Yao, W. Wen, X. Zhang and S. Wang, *Anal. Chim. Acta*, 2019, **1059**, 94-102

[8] F. Liang and Y. Zhu, *Appl. Catal. B Environ*., 2016, **180**, 324-329

[9] Y. Fang, X. Li and X. Wang, *ACS Catal*., 2018, **8**, 8774–8780

[10] D. Jeon, N. Kim, S. Bae, Y. Han and J. Ryu, *ACS Appl. Mater. Interfaces*, 2018, **10**, 8036–804411

[11] Y. Fang, Y. Xu, X. Li, Y. Ma and X. Wang, *Angew.Chem*., 2018, **130**, 9897–9901

[12] J. Wang, L. Xu, T. Wang, S. Chen, Z. Jiang, R. Li, Y. Zhang and T. Peng, *Adv. Funct. Mater*., 2021, **31**, 2009819

[13] Z. Chen, J. Wang, S. Zhang, Y. Zhang, J. Zhang, R. Li and T. Peng, *ACS Appl. Energy Mater*., 2019, **2**, 5665–5676

[14] M. F. Zhu, N. Li and J. S. Ye, *Electroanalysis*, 2012, **24**, 1212-1219.

[15] H. Wu, S. H. Fan, X. Y. Jin, H. Zhang, H. Chen, Z. Dai and X. Y. Zou, *Anal. Chem.*, 2014, **86**, 6285-6290.

[16] Z. N. Yu, L. Zou, Y. L. Chen and J. Z. Jiang, *ACS Appl. Mater. Interfaces*, 2016, **8**, 30398-30406.

[17] Y. X. Wang, M. T. Zhao, J. F. Ping, B. Chen, X. H. Cao, Y. Huang, C. L. Tan, Q. L. Ma, S. X. Wu, Y. F. Yu, Q. P. Lu, J. Z. Chen, W. Zhao, Y. B. Ying and H. Zhang, *Adv. Mater.* 2016, **28**, 4149-4155.

[18] Z. Y. Yu, H. J. Li, X. M. Zhang, N. K. Liu and X. Zhang, *Talanta*, 2015, **144**, 1-5.

[19] B. Xue, K. Z. Li, S. Y. Gu, L. L. Zhang and J. H. Lu, *Sensors. Actuators B Chem*, 2018, **262**, 828.

[20] S. Chen, X. Hai, X. W. Chen and J. H. Wang, *Anal. Chem.*, 2014, **86**, 6689–6694.

[21] Q. Y. Liu, P. P. Chen, Z. Xu, M. M. Chen, Y. N. Ding, K. Yue, J. Xu, *Sens. Actuators B Chem*, 2017, **251**, 339-348.

[22] Y. L. He, N. Li, W. K. Li, X. X. Zhang, X. Zhang, Z. X. Liu, Q. Y. Liu, *Sens. Actuators B Chem*, 2021, **326**, 128850.

[23] Q. Z. Han, H. Y. Wang, D. Wu and Q. Wei, *Biosens. Bioelectron*, 2021, **173**, 112803.

[24] B. Çakıroğlu and M. Özacar, *Biosens. Bioelectron*, 2019, **141**, 111385.

[25] P. P. Wang, L. Cao, Y. Chen, Y. Wu and J. W. Di, *ACS Appl. Nano Mater*, 2019, **2**, 2204–2211.

[26] Y. Wang, Y. X. Cheng, N. Wu and Z. H. Zhang, *ACS Appl. Nano Mater*, 2020, **3**, 8598–8603.

[27] J. Shu, Z. L. Qiu, Q. Zhou, Y. X. Lin, M. H. Lu and D. P. Tang, *Anal. Chem*., 2016, **88**, 2958–2966.

[28] H. Sagura, S. Komathia, M. A. Khan, A. G. Gurek, A. Hassan, *Biosens. Bioelectron*, 2017, **92**, 638-645.

[29] S. Chaiyo, E. Mehmeti, W. Siangproh, T. L. Hoang, H. P. Nguyen, O. Chailapakul, Kurt. Kalcher, *Biosens. Bioelectron*, 2018, **102**, 113-120.

[30] H. Sagura, K. Shanmuga Sundaram, E. N. Kaya, M. Durmuş, T. V. Basovad, A. Hassan, *Biosens. Bioelectron*, 2019, **139**, 111323

[31] J. Ghosh, R. Ghosh and P. K. Giri, *Sens. Actuators B Chem*, 2018, **254**, 681-689.

[32] X. C. Xu, X. H. Niu, S. W. Wu, X. B. Zou and J. M. Pan, *Sens. Actuators B Chem*, 2018, **268**, 430-437.

[33] Z. J. Yang, Y. Tang, J. Li, Y. C. Zhang and X. Y. Hu, *Biosens. Bioelectron*, 2014, **54**, 528-533.

[34] J. J. Jiang, D. Chen and X. Z. Du, *Sens. Actuators B Chem*, 2017, **251**, 256-263.

[35] K. Zhao, W. Gu, S. S. Zheng, C. L. Zhang and Y. Z. Xian, *Talanta*, 2015, **141**, 47-52.

[36] L. P. Lin, X. H. Song, Y. Y. Chen, M. C. Rong, T. T. Zhao, Y. R. Wang, Y. Q. Jiang and X. Chen, *Anal Chim Acta*, 2015, **869**, 89-95.

[37] Y. Huang, M. T. Zhao, S. K. Han, Z. C. Lai, J. Yang, C. L. Tan, Q. L. Ma, Q. P. Lu, J. Z. Chen, X. Zhang, Z. C. Zhang, B. Li, B. Chen, Y. Zong and H. Zhang, *Adv. Mater.*, 2017, **29**, 1700102.

[38] M. Chen, H. Zhou, X. K. Liu, T. W. Yuan, W. Y. Wang, C. Zhao, Y. Y Zhao, F. Y. Zhou, X. Wang, Z. G. Xue, T. Yao, C. Xiong and Y. E. Wu, *Small,* 2020, **16**, 2002343.

[39] L. Zhang, Y. F. Ruan, Y. Y. Liang, W. W. Zhao, X. D. Yu, J. J. Xu and H. Y. Chen, *ACS Appl. Mater. Interfaces*, 2018, **10**, 3372–3379.

[40] S. Zhen, G. C. Fan, Z. M. Li, F. X. Gao and X. L. Luo, *Anal. Chem*., 2018, **90**, 10681–10687.

[41] Y. X. Wen, S. G. Liu, B. X. Tao, H. Q. Luo and N. B. Li, *Sensors Actuators B Chem*, 2020, **304**, 1272796.

[42] L. Zhang, Y. F. Ruan, Y. Y. L, W. W. Zhao, X. D. Yu, J. J. Xu and H. Y. Chen, *ACS Appl. Mater. Interfaces*, 2018, **10**, 3372-3379.